

Supporting Information

Switching Light with Light – Advanced Functional Colloidal Monoalyers

Karina Bley¹, Nina Sinatra¹, Nicolas Vogel^{1,2}, Katharina Landfester¹, Clemens K. Weiss^{1,3}*

¹Max Planck Institute for Polymer Research, Ackermannweg 10, 55128 Mainz, Germany

²School of Engineering and Applied Sciences, Harvard University, McKay 317, 9 Oxford Street, Cambridge, MA 02138 (USA).

³Universtiy of Applied Sciences Bingen, Berlinstrasse 109, 55411 Bingen

SI 1 Scanning electron micrographs of the particles prepared by miniemulsion polymerization and seeded emulsion polymerization

SI 2 Fluorescence emissions spectra of the primary colloidal dispersions and the development of PMI's emission during UV-light and VIS-light irradiation

SI 3 Calculations for the size of the interstitial sites of the template colloids and geometric evaluation of the possible assignment of seeded particles

SI 4 Optical fluorescence micrographs for the photoswitching of a functional colloidal monolayer

This material is available free of charge via the internet at <http://www.pubs.rsc.org>

SI 1: Scanning electron micrographs of the particles prepared by miniemulsion polymerization and seeded emulsion polymerization

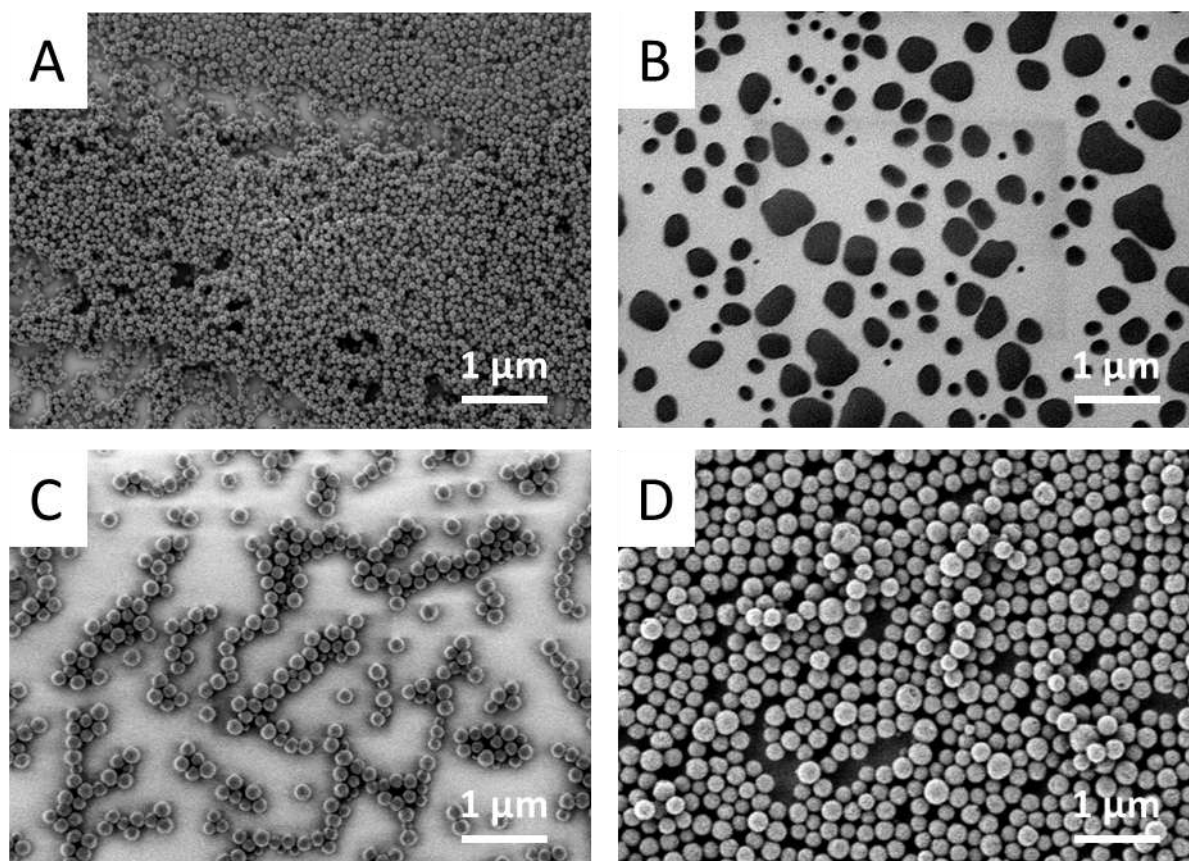


Figure S11. Scanning electron microscopy images of primary colloids prepared by miniemulsion polymerization A) poly(styrene) (PS, $d = 84 \pm 14$ nm), B) poly(butyl acrylate) (PBA, $d = 159 \pm 20$ nm) and colloids produced by seeded emulsion polymerization of the primary colloids C) PS-PS ($d = 191 \pm 17$ nm) and D) PBA-PS ($d = 260 \pm 31$ nm) on silicon substrates.

SI 2: Fluorescence emissions spectra of the primary colloidal dispersions and the development of PMI's emission during UV-light and VIS-light irradiation

A similar decrease of the fluorescence intensity as shown for the primary colloids (Figure SI2) can be detected for the secondary seeded colloids having only lower emission intensity. Upon irradiation with VIS-light the fluorescence of PMI increases which results in a similar course of the emission intensity as for the UV-light irradiated dispersions (Figure SI3).

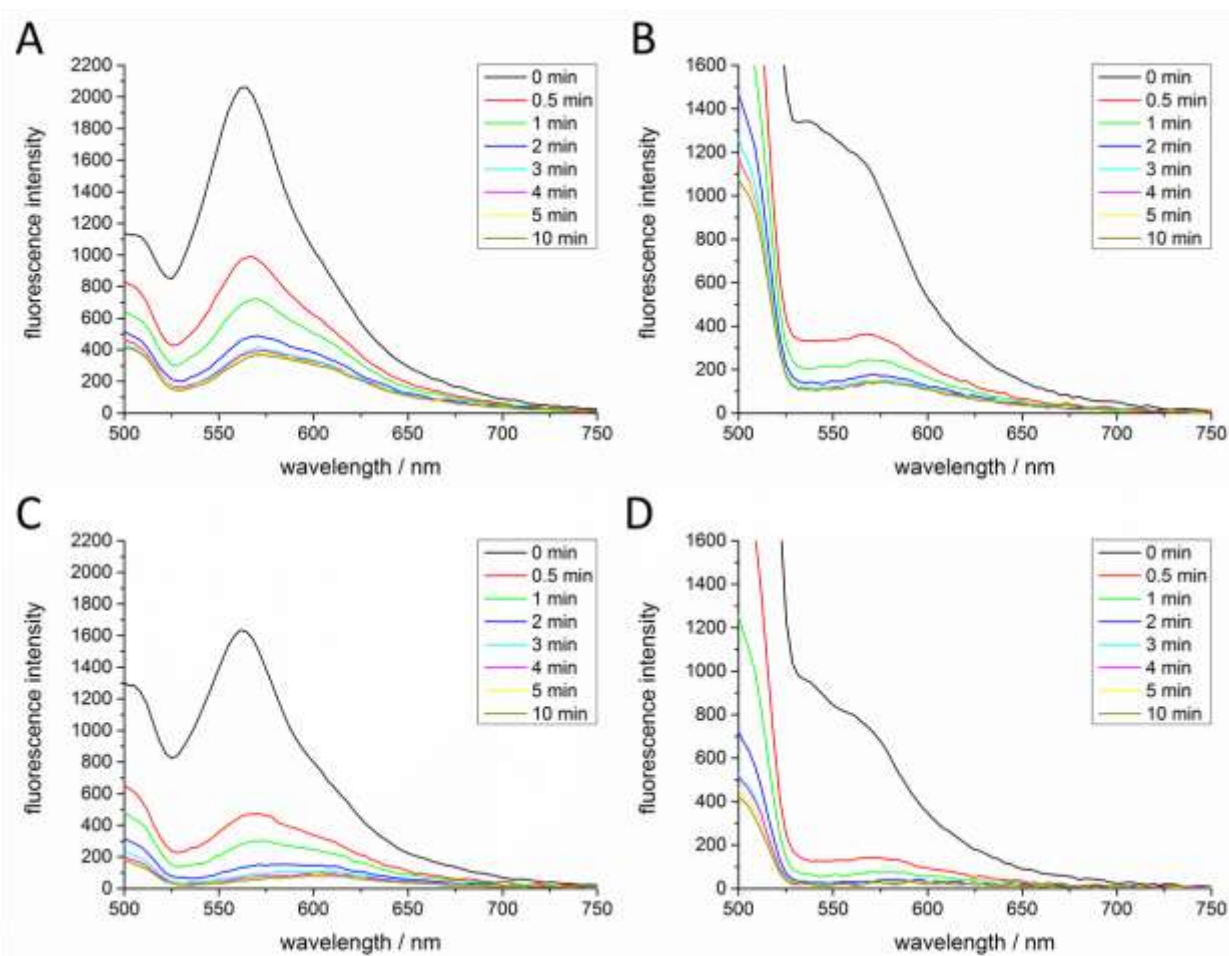


Figure SI2. Emission spectra diagrams the time dependent decrease of PMI's emission during UV-light irradiation for primary colloidal dispersions with 1.5 wt.% solid content for A) polystyrene particles containing the dyes in a ratio of PMI:CMTE as 1:18, B) poly(butyl acrylate) colloids containing the dyes in a ratio of PMI:CMTE as 1:18, C) polystyrene particles containing the dyes in a ratio of PMI:CMTE as 1:37, D) poly(butyl acrylate) colloids containing PMI:CMTE in a ratio of 1:37.

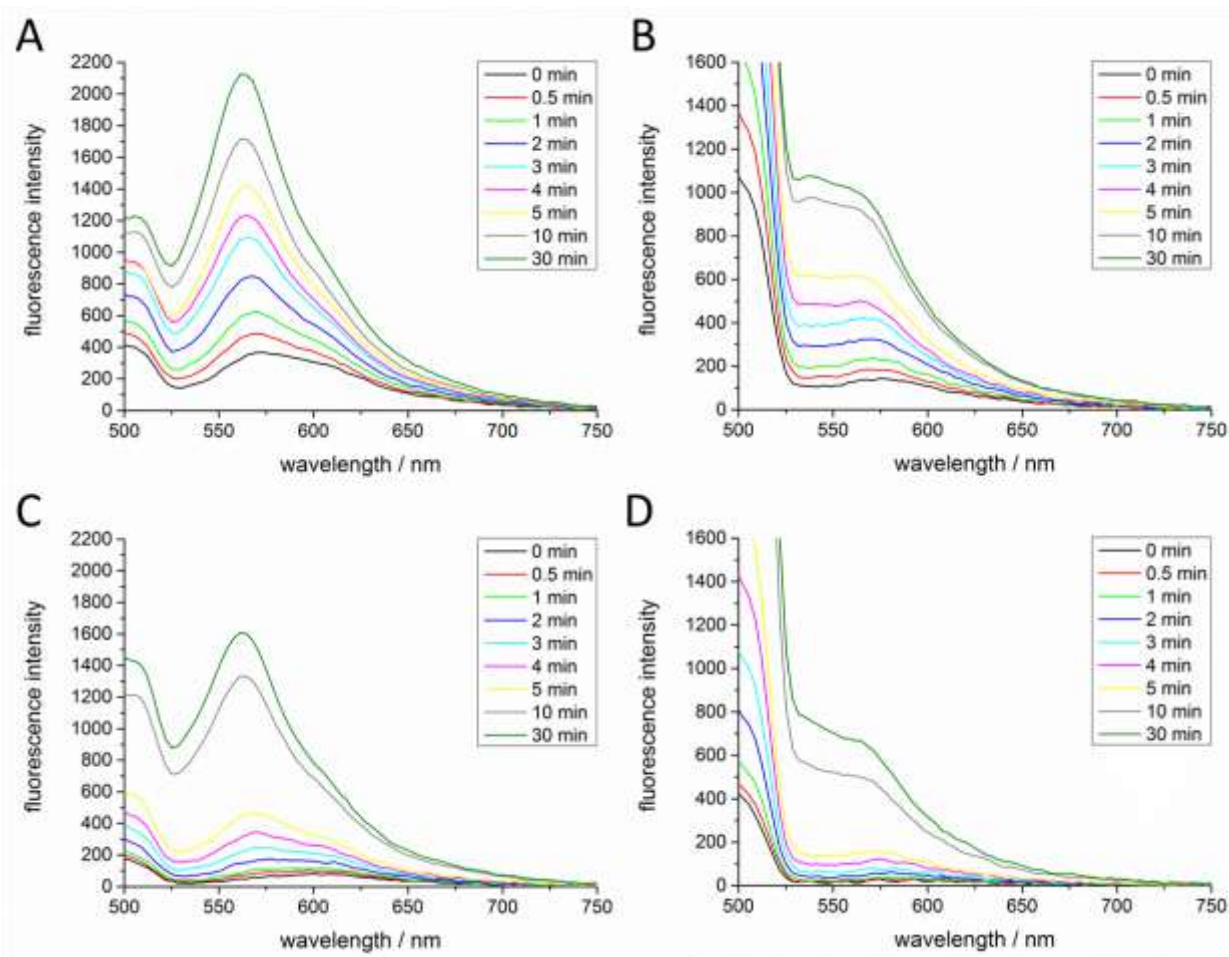


Figure S13. Emission spectra diagrams the time dependent increase of PMI's emission during VIS-light irradiation for primary colloidal dispersions with 1.5 wt.% solid content for A) polystyrene particles containing the dyes in a ratio of PMI:CMTE as 1:18, B) poly(butyl acrylate) colloids containing the dyes in a ratio of PMI:CMTE as 1:18, C) polystyrene particles containing the dyes in a ratio of PMI:CMTE as 1:37, D) poly(butyl acrylate) colloids containing PMI:CMTE in a ratio of 1:37.

SI 3: Calculations for the size of the interstitial sites of the template colloids and geometric evaluation of the possible assignment of seeded particles.

The size of the interstitial sites depends on the contact angle of the colloids at the air-water interface and the immersion depth. If the particles had a hypothetical contact angle of 0° (Figure SI3A), they would be completely immersed in the aqueous phase of the air-water interface. This scenario is physically impossible because the particles will not adhere to the air-water interface. It provides, however, the hypothetical upper limit for the area/volume in the interstitials. For a contact angle $\theta = 90^\circ$ (Figure SI3B) the colloids are half immersed in the aqueous phase with a depth in the range of the particle radius. Thus, the gap size for the small particles is minimal. If the contact angle for the large particles differs from the min or max case the profile of the interstitial site changes (Figure SI3C).

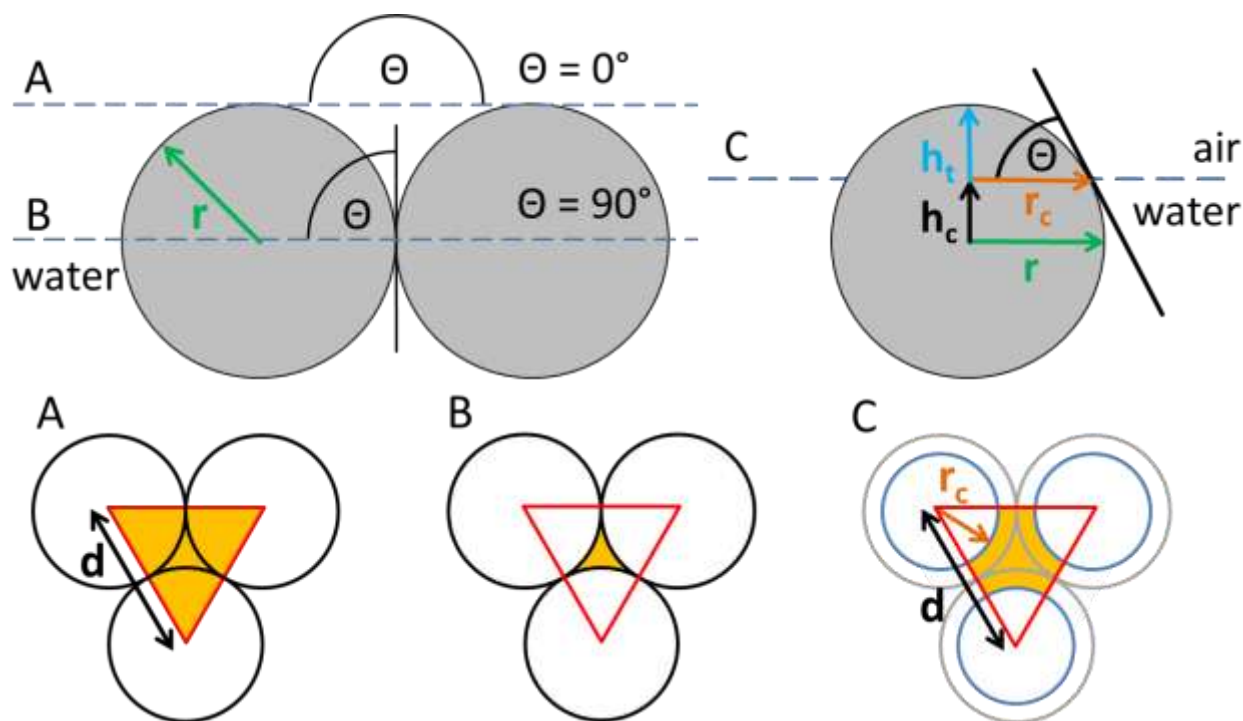


Figure SI4. Determination of the size for the interstitial sites' area (orange) of binary monolayers provided by the large particles at the air-water interface depending on the contact angle θ : A) $\theta = 0^\circ$, colloids are completely immersed into the aqueous phase yielding the maximum area for the smaller particles to be located at, B) $\theta = 90^\circ$, the particles are half immersed with the depth in the range of particle radius yielding the minimum area for the small particles, C) θ between 0 to 90° , the particles are partly immersed into the aqueous phase.

Here, r is the radius, d the diameter, θ the contact angle, r_c the radius of the particles with a contact angle $0 < \theta < 90^\circ$ and an immersion depth h_c and h_t as the part of the large colloids which

reaches out of the aqueous phase. The height h_t at a given contact angle e. g. of 40° for partially immersed particles can be calculated using eq. 1. At a given contact angle of 40° the height h_c is about

$$h_c = r \cos \theta = 440 \text{ nm} \quad (1)$$

$$h_t = r - h_c = 135 \text{ nm} \quad (2)$$

$$r_c = \sqrt{2rh_t - h_t^2} = 370 \text{ nm} \quad (3)$$

The new profile of the interstitial sites, where the smaller seeded particles are located, can be described as a triangular area whereas the corners were cut off by circular segments with radius r_c . (Figure SI5).

$$x = d - 2r_c = 410 \text{ nm} \quad (4)$$

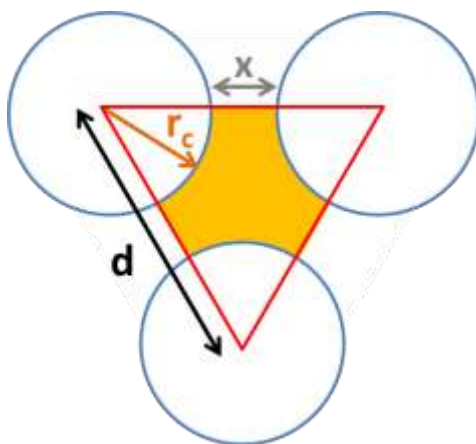


Figure SI5. Sketch for the area of the interstitial sites partially immersed into the aqueous phase at the air-water interface with radius r_c , diameter d and distance x depending on the contact angle of the colloids.

The evaluation for the possible particle assignments of the seeded particles at the interstitial sites was made geometrically. As the particles have a size distribution of about 9% for the seeded polystyrene particles and 12% for the seeded poly(butyl acrylate) particles the standard deviation σ of the Gaussian fit for the determination of the particle size can be used to describe the particle sizes as s (diameter $d-\sigma$), m (d) and L (diameter $d+\sigma$) measured by photon cross correlation spectroscopy. The occurring arrangements were analyzed using the scanning electron micrographs of the binary colloidal monolayer for both hybrid particle systems. The most frequently occurring arrangements are shown in Figure SI6 for seeded poly(butyl acrylate) and in

Figure SI7 for the seeded polystyrene particles. As can be seen even broadly distributed colloids can be arranged at the interstitial site of larger template particles in a binary colloidal monolayer precisely and without disturbance of the self-assembly of the larger particles.

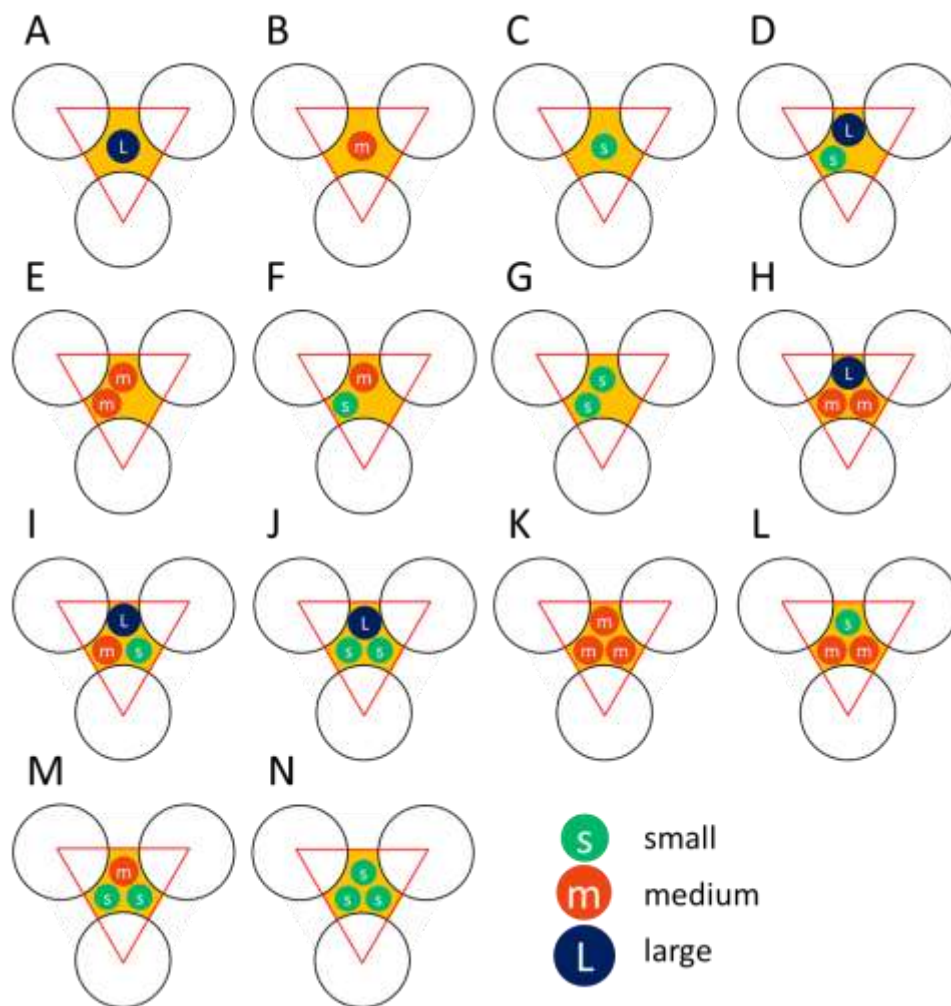


Figure SI6. Observed arrangements for the small seeded poly(butyl acrylate) particles at the interstitial sites of partially immersed larger colloids ($d = 1150$ nm) co-assembled as a binary monolayer A, B and C) for one particle of size s, m and L, D to G) for two particles with all sizes and in combination with a hole. H to N) for three particles at the interstitial site as combinations of all occurring sizes.

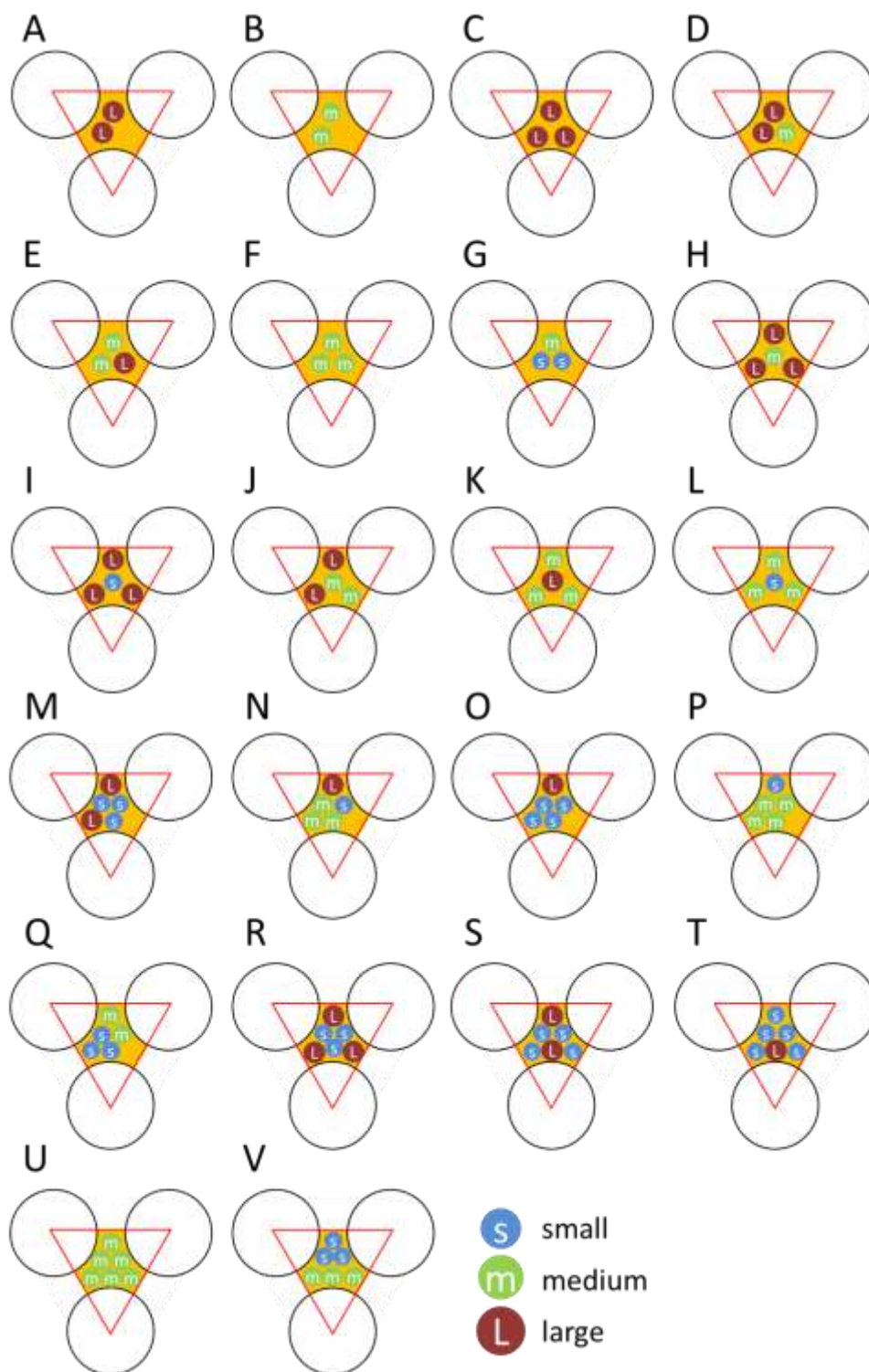


Figure S17. Observed arrangements for the small seeded polystyrene particles at the interstitial sites of partially immersed larger colloids ($d = 1150$ nm) co-assembled as a binary monolayer A and B) for two particles of size m and L, C to G) for three particles as single particle sizes or in combination, H to L) for four particles at the interstitial site as combinations of all occurring sizes, M to Q) for five particles in combination with a hole and R to V) for six particles of single size or in combination.

Geometrical considerations of the resulting colloidal monolayers of the seeded particles located at the interstitial sites of the larger template particles show a distribution of favored colloid arrangements (3 colloids per interstitial site) as determined by the adjusted number ratio $N_{\text{large}}/N_{\text{small}}$ (1:6). Figure SI 8A and B give an overview about the prevalence of the resulting colloidal arrangements obtained from an evaluation of the number of colloids in the interstitial positions from the micrographs of the binary monolayers (Fig 7A and 7B)

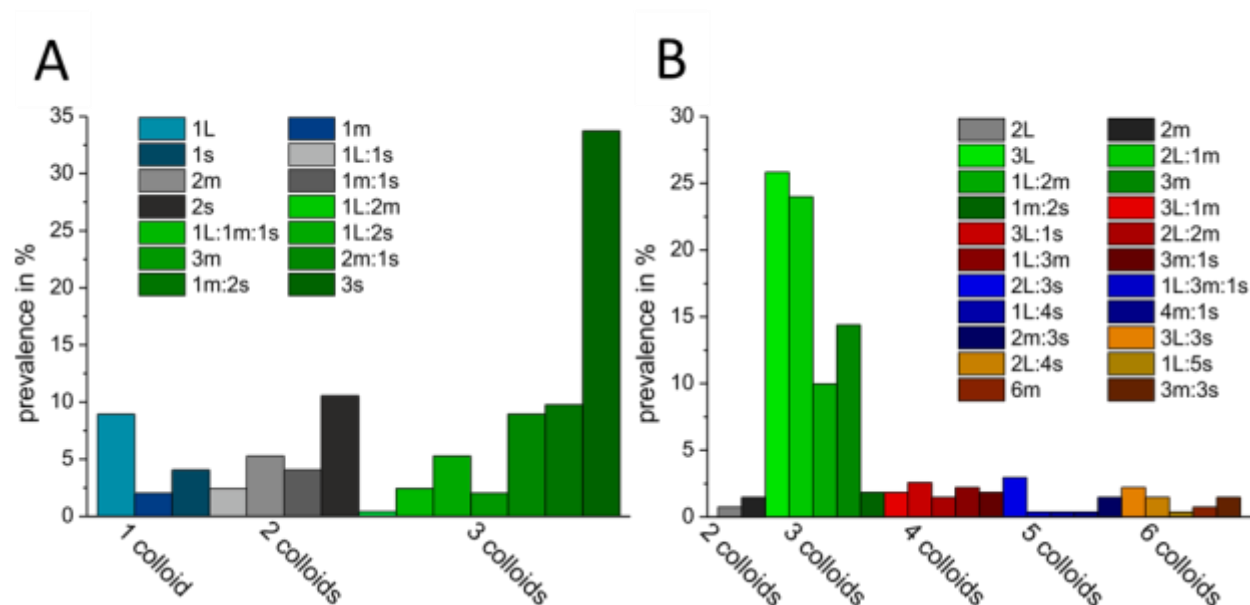


Figure SI8. A) Statistical analysis of the functional binary colloidal monolayers for the possible arrangements of the smaller PBA-PS (Fig 7B) colloids located at the interstitial positions with a prevalence of 3 colloids (63%) and B) statistical analysis of the possible arrangements for the smaller PS-PS (Fig 7A) colloids with max. 6 colloids (6%) and a prevalent arrangement of 3 colloids (76%) located at the interstices.

SI 4: Optical fluorescence micrographs for the photoswitching of a functional colloidal monolayer

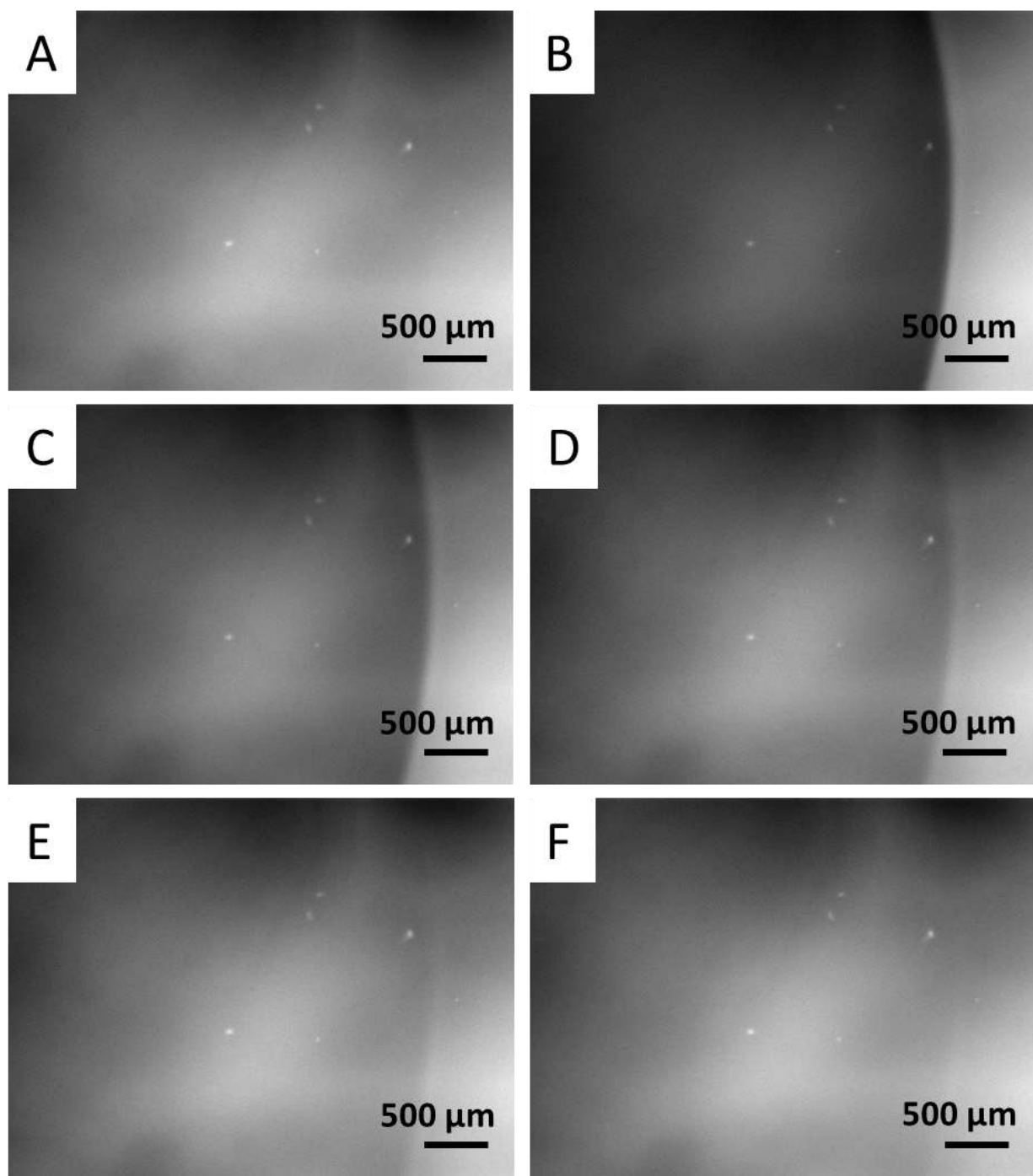


Figure SI9. Optical micrographs of a monolayer from photoswitchable PBA colloids using a fluorescence microscope with an 2.5x objective and different optical filters (DAPI-filter, $\lambda_{ex} = 360$ nm and $\lambda_{em} = 420$ nm and eGFP-filter, $\lambda_{ex} = 472$ nm and $\lambda_{em} = 520$ nm) (A) after irradiation with VIS-light for 5 min using the eGFP-filter, (B) after irradiation with UV-light for 5 min using the DAPI-filter (circular part of the monolayer), (C) after excitation with VIS-light at $\lambda_{ex} = 472$ nm for 120 ms (eGFP-filter), (D) after excitation for 180 ms, (E) after excitation for 240 ms and (F) after excitation for 300 ms.